JEE Journal of Ecological Engineering

Journal of Ecological Engineering 2024, 25(7), 305–316
https://doi.org/10.12911/22998993/188879
ISSN 2299–8993, License CC-BY 4.0

Received: 2024.05.03
Accepted: 2024.05.23
Published: 2024.06.01

The Effects of Ozonolysis on Oil Palm Fruit Mesocarp Delignification

Asyeni Miftahul Jannah Asyeni[1,2*], Muhammad Faizal[1], Novia Novia[1], Hary Widjajanti[3]

[1] Faculty of Engineering, Universitas Sriwijaya, Palembang 30139, South Sumatra, Indonesia

[2] Chemical Engineering Department, Faculty of Engineering, Universitas Sriwijaya, Jl. Raya Palembang-Prabumulih KM. 32 Ogan Ilir 30662, South Sumatra, Indonesia

[3] Biology Department, Faculty of Mathematics and Natural Sciences, Universitas Sriwijaya,Ogan Ilir 30662, South Sumatra, Indonesia

* Corresponding author's email: asyeni@ft.unsri.ac.id

ABSTRACT

Oil palm fruit mesocarp (OPFM) is a solid by-product containing cellulose, potentially serving as a raw material for biofuel. The cellulose content of this solid by-product can be extracted through delignification. Therefore, this study aimed to investigate the application of ozone for OPFM delignification to break down lignin bonds in the material. During the analysis, ozonolysis delignification was influenced by particle size, oxygen flow rate, and reaction time. Ozone flowrate analyzed using the Iodometric method. Cellulose, hemicellulose, and lignin content of raw material and treated samples were analyzed using the α – cellulose, γ – cellulose, and the Kappa method. The results showed that by using a particle size of 100 mesh, and a flow rate of 2 $Lmin^{-1}$ for 15 min, ozone degraded 42.03% lignin, 15.89% hemicellulose, and concentrated 62.85% cellulose. SEM and FTIR results showed the removal of hemicellulose and lignin from OPFM with ozonolysis delignification. Furthermore, XRD analysis showed the crystallinity degree of the high cellulose yield.

Keywords: oil palm fruit mesocarp, ozonolysis delignification, particle size, oxygen flow rate, reaction time.

INTRODUCTION

Oil palm fruit mesocarp (OPFM) is a solid waste from oil palm production, posing a significant environmental challenge. The palm oil industry produces a lot of OPFM as waste. Generally, these industries utilize OPFM only as fuel for boilers and are not fully utilized. Combusted OPFM causes environmental impacts without any more economical and sustainable utilization. Currently, Indonesia is the world's largest oil palm producer, exporting 55.6% of global palm oil demand by 2023 (United State Department of Agriculture, 2023). OPFM contains 60% cellulose, a potential source of biofuel, 17.9% hemicellulose, and 11% lignin (Simão et al., 2019; Sreekala et al., 1997). Cellulose is a renewable energy source that can be converted into glucose and fermented into bioethanol. However, the presence of lignin content requires delignification as the upper layer of lignocellulose covers the cellulose bonds, inhibiting the conversion ability of the catalyst. This shows that delignification accelerates cellulose hydrolysis, where the rate of lignin removal corresponds with the process efficiency. In this study, the delignification process uses the ozonolysis method by including ozone (O_3) as a catalyst to oxidize, dissolve, and destroy the lignocellulose cell wall (Keris-Sen and Gurol, 2017). Initially, ozone gas is flowed into ozonolysis reactor filled with OPFM, playing an effective role without producing toxic waste or damaging the structure of cellulose and hemicellulose during delignification process (Mardawati et al., 2018). Additionally, ozone is a strong oxidant and highly reactive in degrading lignin (Kamel et al., 2015), which is considered a clean and environmentally friendly technology (Sulfahri et al., 2020) capable of breaking cellulose bonds in biomass without including harmful chemicals (Wan and Saidina, 2021).

Based on these advantages, ozonolysis method is considered suitable for degrading lignin.

Ozone that is widely used in the delignification process is generated from the conversion of oxygen using an ozone generator. Furthermore, it flows into a fixed bed reactor containing OPFM mixed with distilled water to optimize the reaction between raw material particles and minimize waste (Bhattarai et al., 2015). this study, ozone was produced using a corona discharge ozone generator with model AZ-1000MG-G, 220 V/50 Hz AC voltage source. It is capable of converting oxygen into ozone with oxygen sourced from pure oxygen as input. The input flow is connected to an oxygen supply tube that has been equipped with a flowmeter. Therefore, the flow rate of the input oxygen can be adjusted or varied to achieve the optimum flow rate. Ozone production was analyzed using the Iodometric method. During the delignification process, ozone comes into contact with OPFM in an ozonolysis reactor, with particle size significantly influencing the contact area of ozone to the sample. The particle size of tiny samples can simplify ozone to degrade lignin, showing the need for physical treatment before the delignification process. This study aimed to analyze the effects of ozonolysis delignification on lignin degradation to enhance concentrate cellulose. Therefore, the contents of cellulose, hemicellulose, and lignin were analyzed before and after delignification in this study. Specifically, cellulose, hemicellulose, and lignin content were analyzed using the α-cellulose, γ-cellulose, and the Kappa method, respectively. SEM, FTIR, and XRD analyses were also conducted to analyze the effect of ozone delignification on OPFM.

MATERIALS AND METHODS

Materials

OPFM as raw material was collected from Bangka, Indonesia. The samples collected were cleaned and dried to reduce the moisture content, followed by cutting into small pieces to facilitate the pulverization process and blending to reach the size of 80 mesh and 100 mesh. The pro-analyst chemicals used included NaOH, distilled water, potassium dichromate, H_2SO_4, ferroin indicator, ferrous ammonium sulfate, $KMNO_4$, KI, sodium thiosulfate, and amylum.

Ozonolysis delignification

OPFM powder was weighed for 5 g each and wetted with 10% H_2O by weight of the material pH of 3 (Hermansyah et al., 2021). The wetted sample was put into the ozone reactor and the flow rate was adjusted with variations of 1 $Lmin^{-1}$, 2 $Lmin^{-1}$, and 3 $Lmin^{-1}$. The reaction time variation in the ozone reactor was varied for 5 min, 10 min, and 15 min, followed by connecting the power cord to the ozone generator. Initially, the voltage regulator was set to the lowest point (zero), to maintain low voltage (220 V). The oxygen gas flow rate was adjusted as required and kept stable. This was followed by a gradual increase of mains voltage until an intended value was reached. Before ozonizing the biomass, ozone content was measured by the iodometric method and a 2% KI solution was put into the first analysis vessel. During the bubbling stage, ozone-containing gas was poured into the analysis tube and the flow of ozone-containing gas was stopped. Subsequently, a portion of the solution present in the analysis tube was titrated with $Na_2S_2O_3$ solution using a starch indicator. Ozone that did not react in the reactor flowed into the second analysis vessel filled with 2% KI solution. The ozone content of ozonation reaction was analyzed as in the first analysis vessel using the Iodometric method. The delignified sample was soaked with 100 mL of 5% NaOH at room temperature for 60 min, filtered, and spelled with hot aquadest until the pH was neutral. Furthermore, each sample was dried using ovens for 24 hours at 105 ºC to achieve 0% moisture content.

Ozone production analysis

The 200 mL KI solution that passed through ozone was added with 10 mL H_2SO_4 to form a darker-colored solution, followed by the immediate addition of H_2SO_4 and titrated with 0.2 N $Na_2S_2O_3$. Furthermore, 0.5 ml of 2% amylum was added after the color turned pale yellow, causing the solution to turn dark blue. The titration was continued until the color changed colorless and the volume of $Na_2S_2O_3$ was measured. The formula used to compute the ozone concentration of the sample solution is expressed as follows:

$$Ozone\ formed = \\ = \frac{24 \times Na_2S_2O_3\ Volume\ (mL) \times Na_2S_2O_3\ Normality}{Inlet\ gas\ volume\ (mL)} \quad (1)$$

SEM, FTIR, and XRD analysis

The raw material and product were examined using a Tescan Vega 4 LMH scanning electron microscope to obtain the surface morphology. Furthermore, the samples were examined using a Prestige 21 FTIR instrument in the range of 500–4000 cm^{-1} to show the absorption band of cellulose, hemicellulose, and lignin. X-ray diffraction was used to show the high amount of cellulose structure, and determine crystallinity degree as well as particle size.

RESULTS AND DISCUSSION

The effect of oxygen flow rate and reaction time on ozone production

Oxygen as feedstock was fed into the ozone generator, producing ozone, which flowed to the analyzer column. This column was filled with KI solution and ozone was dissolved in KI. To achieve optimum production, variations were made to the flow rate and reaction time. The oxygen flow rate used varied at the rates of 1, 2, and 3 $Lmin^{-1}$ with variations in reaction time of 5, 10, and 15 min. As shown in Figure 1, the highest ozone concentration produced was 9.56 mg/L at a reaction time of 15 min with an oxygen flow rate of 1 $Lmin^{-1}$. The longer ozonolysis time caused more ozone to form, which was abundant at a smaller oxygen (O_2) flow rate of 1 $Lmin^{-1}$. This phenomenon was attributed to the equilibrium of the ozone formation process, where the reaction proceeded rapidly because the limiting reagent was the amount of ozone, instead of the oxygen. Increasing the oxygen flow rate can increase the ozone capacity, as more oxygen molecules are available for ozone formation. However, excessive flow rates may result in a lower ozone capacity due to the formation of less reactive ozone species or the generation of unwanted byproducts (Yulianto et al., 2019). Furthermore, the reaction time can significantly impact the ozone concentration and lead to higher energy efficiencies. Longer reaction times generally lead to higher ozone concentrations, as more oxygen molecules have the opportunity to react and form ozone (Shrestha et al., 2015). Regardless of the amount of oxygen in the generator, the quantity of ozone formed depended on

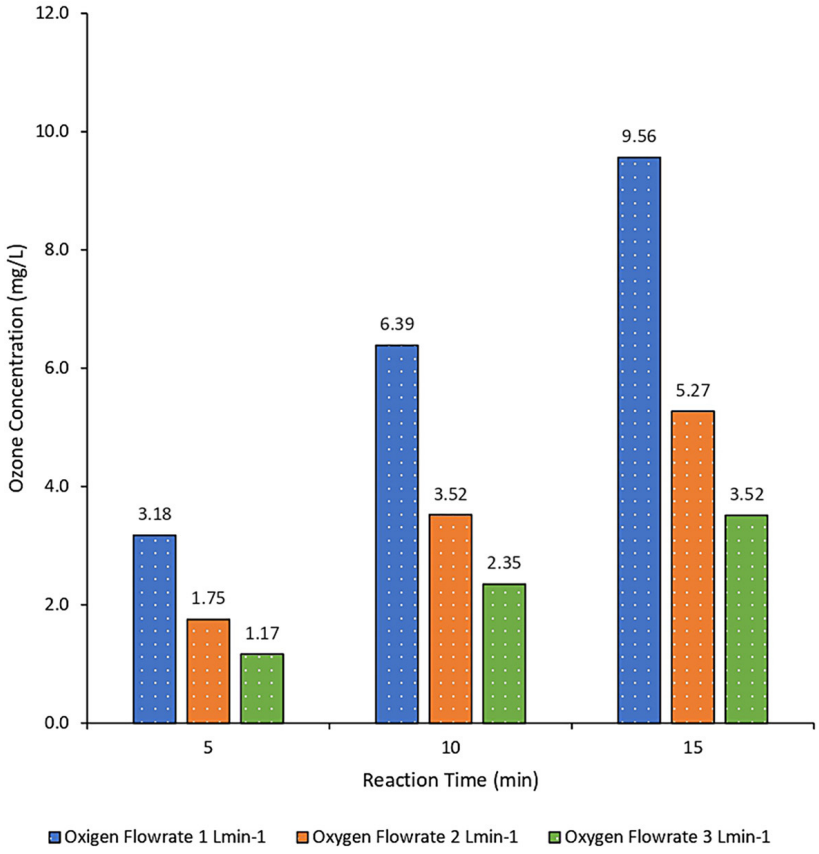

Figure 1. The effect of oxygen flow rate and reaction time on ozone concentration

the availability of potential energy used to convert oxygen at a flow rate of 1 $Lmin^{-1}$.

The effect of ozonolysis delignification on OPFM

OPFM was delignified using ozone with flow rate variations of 1 $Lmin^{-1}$, 2 $Lmin^{-1}$, and 3 $Lmin^{-1}$ for 5, 10 and 15 min. After this process, cellulose, hemicellulose, and lignin content were analyzed, as shown in Table 1. The results showed that the particle size of the sample affected the reduction of lignin content in OPFM, leading to a high amount of cellulose. Furthermore, ozonolysis delignification process was effective in degrading lignin and hemicellulose bonds by 60.21% in the 100-mesh sample for 10 minutes using 2 $Lmin^{-1}$ oxygen. The amount of lignin removed for each sample is shown in Figures 2 to 4, where the maximum degraded content was 45.98% in the 100-mesh sample with an ozone flow rate of 1 $Lmin^{-1}$ for 15 min of reaction. A previous study stated that the amount of biomass surface area when reacting with ozone significantly affected lignin degradation (Rodolfo Travaini et al., 2016).

The results showed that the largest lignin removal was obtained in the sample with a 100-mesh size. The particle size of OPFM has a very significant effect on achieving the optimum ozonolysis process. The smaller particles interact with ozone, making the degradation of lignin becomes more preferable, improving the ability of ozone to break lignin bonds in OPFM, and resulting in reduced surface area. Therefore, ozone reacted more easily with OPFM to break lignin bonds, as observed in a previous study on

Table 1. Cellulose, hemicellulose, and lignin content of OPFM after the ozonolysis delignification process

Particle size (mesh)	Flowrate ($Lmin^{-1}$)	Reaction time (min)	Cellulose (%)	Hemicellulose (%)	Lignin (%)
Untreated	-	-	62.84	17.31	11.07
60	1	5	66.76	9.19	8.96
		10	67.92	10.55	9.81
		15	68.31	8.99	8.99
	2	5	69.16	9.13	9.79
		10	69.98	9.71	9.50
		15	71.12	6.12	9.51
	3	5	70.87	8.33	10.15
		10	70.83	8.88	9.95
		15	71.16	9.32	10.08
80	1	5	63.69	17.19	10.20
		10	63.31	16.94	10.02
		15	65.86	16.11	9.81
	2	5	62.86	16.88	9.59
		10	62.84	17.09	10.58
		15	62.85	16.08	10.02
	3	5	62.86	16.40	9.72
		10	62.88	16.83	9.52
		15	64.20	15.06	9.34
100	1	5	62.91	16.31	9.29
		10	63.11	16.05	9.50
		15	62.87	16.80	9.90
	2	5	62.96	16.74	10.81
		10	62.89	16.55	9.64
		15	62.88	16.89	9.53
	3	5	62.87	16.97	10.65
		10	62.85	17.10	10.38
		15	62.84	16.77	10.09

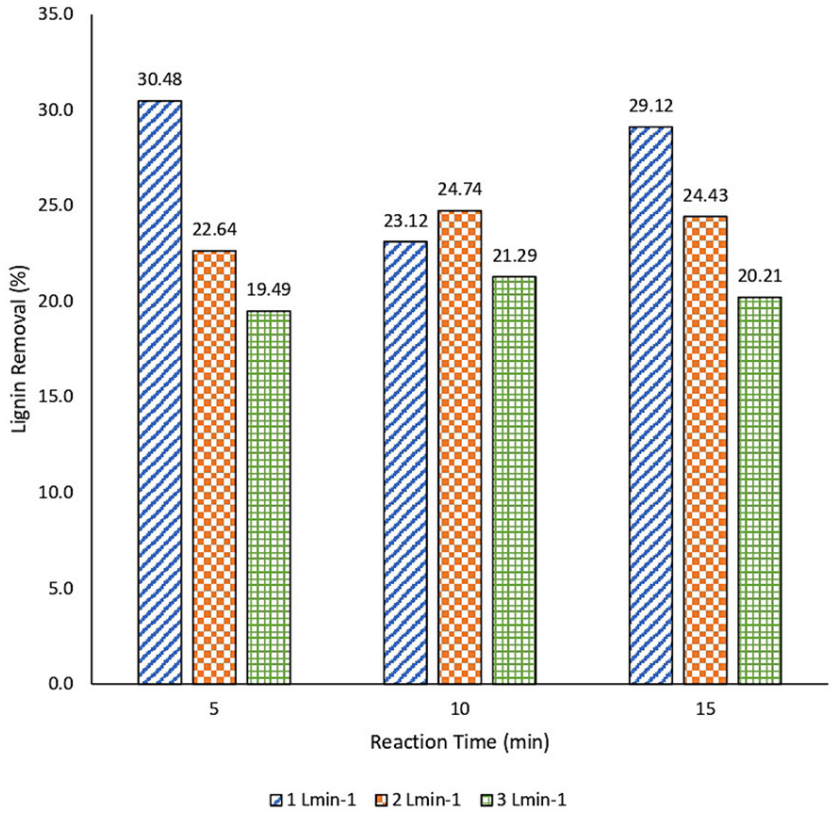

Figure 2. The effect of oxygen flow rate and reaction time on 60 mesh OPFM ozonolysis delignification

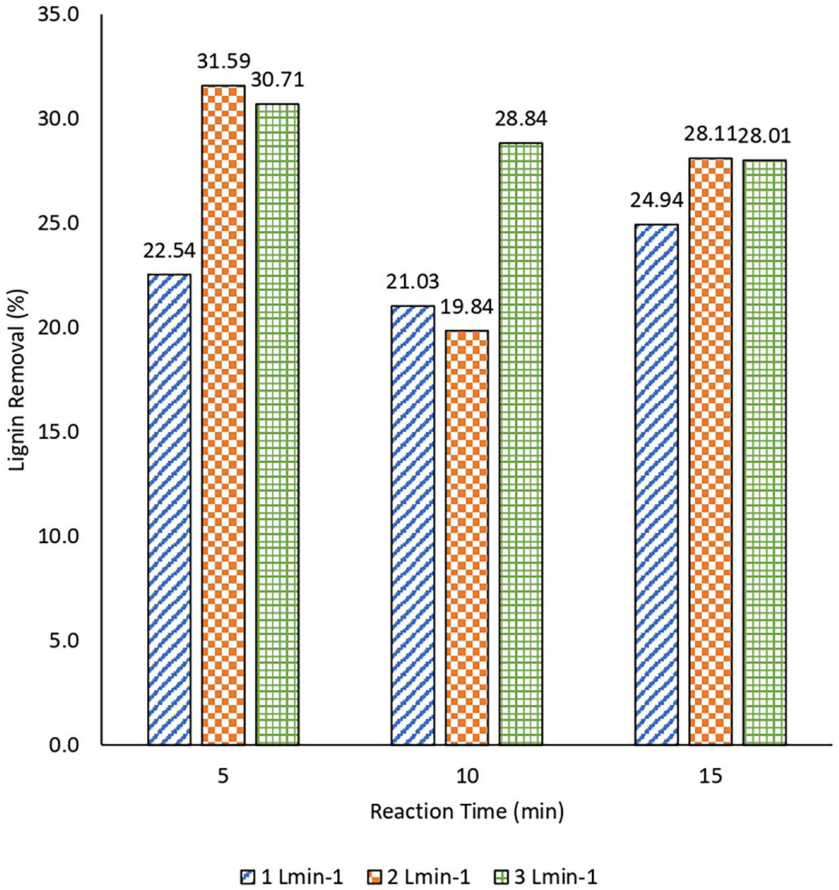

Figure 3. The effect of oxygen flow rate and reaction time on 80 mesh OPFM ozonolysis delignification

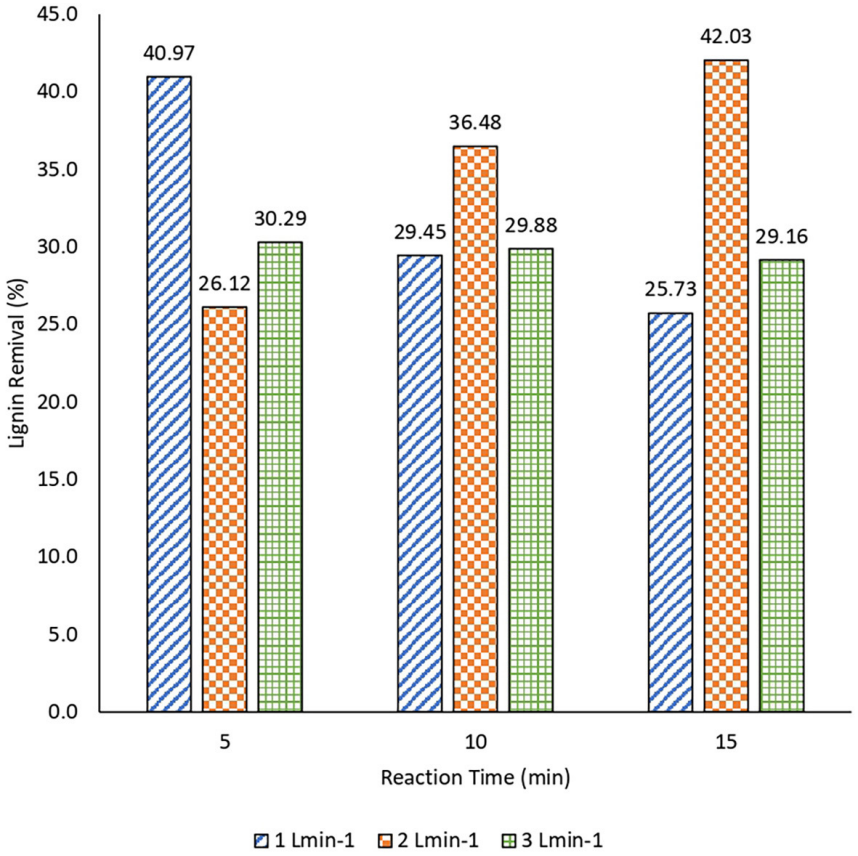

Figure 4. The effect of oxygen flow rate and reaction time on 100 mesh OPFM ozonolysis delignification

palm fronds (Wan and Saidina, 2016). Ozone was able to degrade 87.9% of lignin palm fond in samples with particle sizes of 80 mm or more than 20.6% of those with a size of 50 mm using the same treatment. The study of Shi et al. (2015) applied ozonolysis delignification to maize straw with a size range of 160 to 21 µm. The results showed that ozonolysis delignification was very effective at a particle size of 64 µm as evidenced by the highest glucose yield (Shi et al., 2015). Similar results were also shown in research conducted by Barros et al. (2013) on ozonolysis delignification of sugarcane bagasse and straw. The study concluded that the sample particle size of less than 2 mm can increase yield. The surface area of the sample can affect the results obtained (Barros et al., 2013). Since smaller particle size has better contact with ozone, the reaction between solid particles and ozone can take place more efficiently. Smaller solid particles also tend to have a more uniform size compared to larger size, which affects the distribution in the gas-solid mixture and reactivity during reaction with gas (Sharma and Pugsley, 2007). Li et al. reported similar results on ozonolysis delignification with maize strove. It was discovered that smaller particles are better for ozonolysis (Li et al., 2015).

Furthermore, lignin degradation increases as the amount of ozone reacted increases due to the powerful oxidizing properties of ozone. This is because a higher flowrate can provide a more consistent and intense exposure of ozone to the lignin, leading to a higher rate of radical formation and subsequent lignin degradation (Baig et al., 2015; Anggoro et al., 2022). When lignin comes into contact with ozone, it can be degraded rapidly, leading to the break of aromatic rings and the generation of carboxyl groups (Wan et al., 2021). This process is facilitated by the formation of radicals, which are very reactive species and react close to where lignin was formed. The radicals can degrade cellulose at acidic pH but primarily react with lignin leading to its destruction. Therefore, increasing ozone consumption can generate the lignocellulose structure by breaking lignin bonds (García-Cubero et al., 2009; Rodolfo Travaini et al., 2016) and degrading the carbohydrate bonds in the biomass (Binder et al., 1980). Ozone also interacts with lignin breakdown products, producing aliphatic acids and low

molecular substances, which impede the function of enzymes and reduce glucose yield (Neely, 1984). Ozone mostly dissolved lignin and mildly solubilized the hemicellulose portion, resulting in minimal cellulose loss (Travaini et al., 2015). Lee et al conducted a study on coastal Bermuda grass and observed that a 31.3% increase in the amount of lignin degraded raised the ozone reaction by 26.4% (Lee et al., 2010). The quantity of ozone that reacts determines the influence of reaction time on the ozonolysis process. Therefore, the efficiency of the delignification process will continue to increase until optimum time is reached (Schultz-Jensen et al., 2011).

In this study, the optimum reaction time for ozonolysis delignification was 15 min with 42.03% of lignin removal. The reaction time influences the extent of lignin degradation achieved during the treatment process, with longer reaction times generally leading to more extensive lignin removal (Baig, 2022; Hermansyah et al., 2021). However, this increased the expense of delignification. This study took less reaction time with high lignin removal compared to prior studies. The 50% delignification was accomplished using 2.7% (w/w) wheat straw over a 2 h reaction (García-Cubero et al., 2012). The ozonolysis delignification also treated bagasse sugarcane and yielded 92.5% cellulose after 120 min (Rodolfo Travaini et al., 2013). The ozone delignification reaction involves the insertion of an oxygen atom into carbon-hydrogen bonds, thus disintegrating the lignin structure (Vitasari, 2008). Ozone is highly reactive toward compounds with double bonds and functional groups, making it highly effective in breaking down the complex structure of lignin (M'Arimi et al., 2020). The interaction of ozone with the OPFM surface has a significant impact on the adsorption process due to the chemical and structural changes that occur during the ozonation process. The ozone treatment breaks down the lignin, which is the most outermost layer of the biomass, allowing for better access to the cellulose and hemicellulose components. This increased accessibility enhances the adsorption process by providing a more porous and reactive surface for the adsorbate to bind to (Suhada et al., 2021; Valdés et al., 2002).

SEM analysis

SEM analysis was treated on OPFM samples before and after ozonolysis delignification process. This analysis was carried out to show the difference in morphology of lignin degradation in the sample. Based on the results, the untreated OPFM showed an absence of voids in the sample. Figure 5 shows that OPFM fiber has a hollow top layer

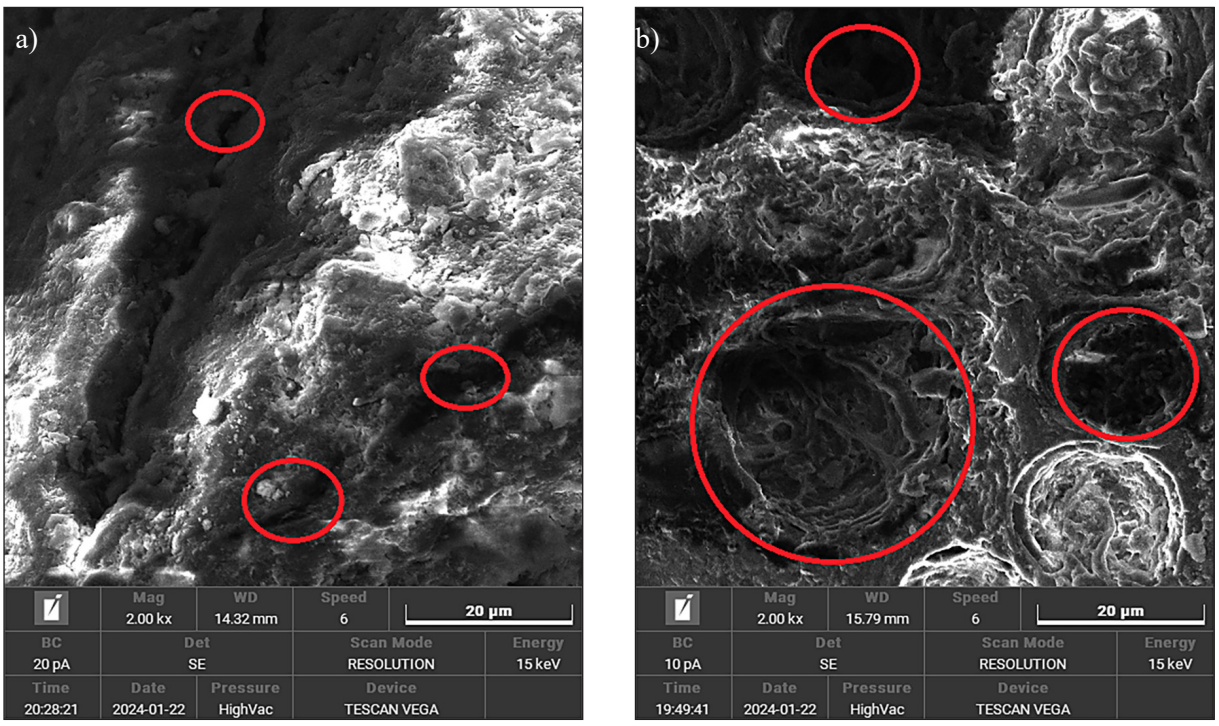

Figure 5. SEM images of OPFM (a) untreated, (b) after-treated

indicating degradation of lignin bonds. This phenomenon showed the loss of lignin bonds wrapping the fiber had been partially lost due to ozonolysis delignification process, exposing the cellulose surface (Lim and Zulkifli, 2018). Additionally, the formation of voids showed the expansion of the inner surface due to missing hemicellulose bonds (Elanthikkal et al., 2010). The asymmetric and smoother appearance of OPFM fiber showed the effectiveness of ozone in degrading lignin and hemicellulose. The composition of untreated and treated OPFM show in Table 2. Based on these compositions, the amount of carbon decreased about 34.91% after ozonolysis pre-treatment, but the amount of oxygen increased about 41.94%. The reduced carbon content after pre-treatment is because a number of carbon bonds contained in lignin and hemicellulose have been degraded. carbon elements that are degraded after the ozonolysis process are dissolved in the washing stage after leaving the ozonolysis reactor. The remaining carbon was the carbon bond contained in the concentrated cellulose. Figure 5 shows the pores in the treated sample which indicates that the top cover layer has been exposed. The sample pores look larger because the hemicellulose content in the treated sample has been reduced and resulted in the formation of larger pore cavities in the treated sample. The dissolving lignin on the surface of the sample after pre-treatment was indicated by the reduction of 34.91% carbon and the oxygen increased by 41.92%, as shown in Table 2. The removed carbon was a lignin constituent component that had been degraded and dissolved in the washing process after the ozonolysis pre-treatment which aimed to neutralize the pH of the sample.

FTIR analysis

OPFM sample was analyzed using FTIR with a range of 500–4000 cm^{-1}, as shown in Figure 6. The results showed strong absorption band ranging from 2800–3400 cm^{-1}, which indicated the presence of hydrogen bond (O-H) absorption at the peak of 3335.69 cm^{-1} (identification of cellulose bonds). Strong intensity of absorption was also observed in the wave range of 3331.59–3335.69 cm^{-1} in charge of absorbing O-H valence vibrational bonds on cellulose intermolecular (Schwanninger et al., 2004). This shows that ozone was able to degrade lignin bonds as the outer layer of lignocellulose well. Strong absorption at the peak of 1030.47 cm^{-1} showed the capacity of the wave to absorb C-H aromatic bond deformation. This showed the presence of symmetrical CH_2 bonds with hydrogen (O-H). IR wave 2849.19 cm^{-1} absorbed valence vibrations of CH_2 bond asymmetry, while at 2916.93 cm^{-1} absorbed valence vibrations of CH_2 symmetry with hydrogen bonds (O-H) (Schwanninger et al., 2004). The strong

Table 2. Compositions of untreated and after treated OPFM

Element	Netto		Mass (%)		Atom	
	Untreated	After treated	Untreated	After treated	Untreated	After treated
Carbon	141,145	91,868	61.95	51.11	68.49	59.12
Oxygen	43,793	62,161	37.85	44.68	31.41	38.80
Silicon	1,463	30,984	0.20	4.21	0.10	2.08

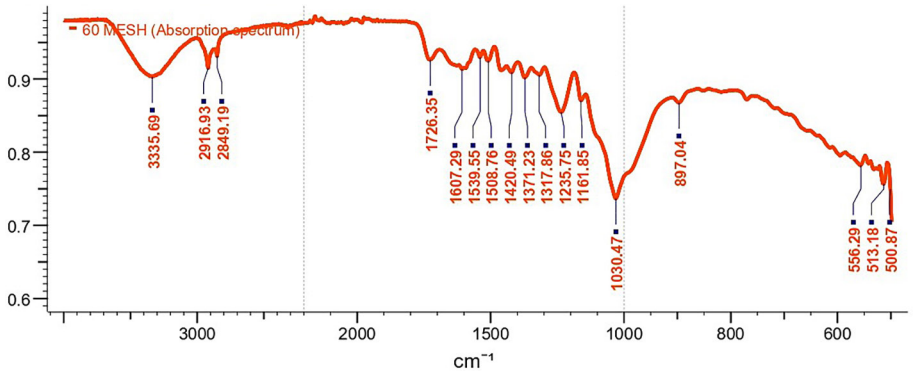

Figure 6. FTIR of treated OPFM

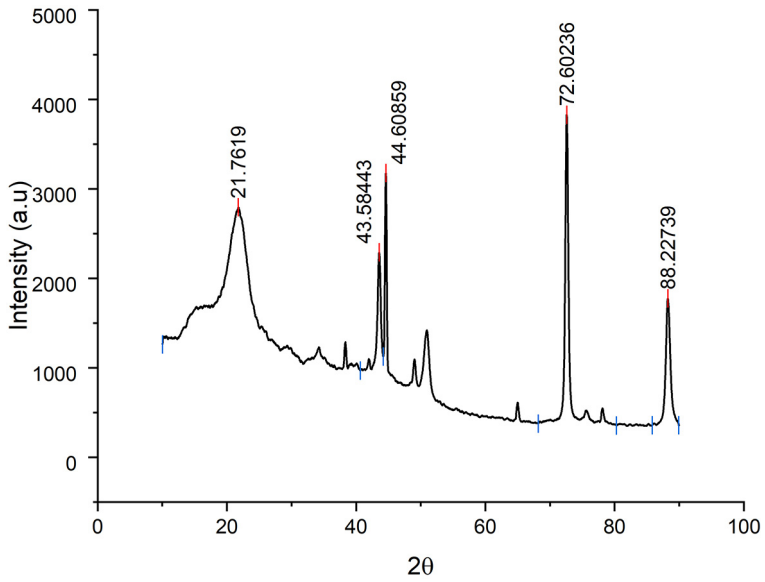

Figure 7. XRD of treated OPFM

intensity of this absorption wave was similar to the IR spectra value of hardwood lignin (Pandey, 1999). This showed that the bonding structure of lignin in OPFM was similar to lignin in hardwood biomass (Isroi et al., 2012). Furthermore, lignin bonds were also visible in the absorption band of 1508.76 cm^{-1}, which showed the presence of C=C vibrations (Faix et al., 1991). The absorption band value of 1161.85 cm^{-1} and 1726.35 cm^{-1} showed the presence of asymmetric C-O-C valence vibrations (Fackler et al., 2010). The wave 1726.35 cm^{-1} absorbed the unconjugated carbonyl bond derived from uronic acid in xylan hemicellulose (Faix et al., 1991). The 897.04 cm^{-1} wave absorbed the C-H-O deformation of the *β*-(1–4)-glycosidic bond (Fackler et al., 2010).

XRD analysis

XRD analysis of OPFM presented in Figure 7 showed that the sample observed has several peaks at 2θ = 21.76, 43.58, 44.61, 72.60, and 88.23. The crystallinity degree of OPFM was 95.94% with a particle size of 56.06 nm. In this study, the crystallinity degree of cellulose obtained was significantly higher compared to the results of Chieng et al. The crystallinity degree of OPFM with NaOH and continued with H_2SO_4 delignification at 80 °C for 4 h was obtained at 77.8% (Chieng et al., 2017). Yasim-Anuar et al. obtained a crystallinity degree of 56% by delignifying OPFM using 5% (w/v) $NaClO_2$ at 70 °C for 90 min (Yasim-Anuar et al., 2017). The high crystallinity degree showed the elevated amount of cellulose structure to the total particles in the sample. The cellulose with higher crystallinity can be more easily processed and recycled, potentially reducing the environmental impact of the production process (Carolin et al., 2023). Furthermore, the higher levels of crystallinity in cellulose enhance mechanical properties, such as strength, flexibility, and resistance to degradation (Vanderfleet and Cranston, 2021).

CONCLUSIONS

In conclusion, this study showed that ozonolysis delignification process on OPFM was effective in degrading lignin. In this treatment, OPFM particle size and oxygen flow rate affected the interaction between ozone and lignocellulose bonds. The results showed that ozone could dissolve in moist lignocellulose and adsorb into particles at smaller particle sizes. In this study, ozone degraded lignin by 42.03% in the 100 – mesh, showing the significant effect of particle size and oxygen flow rate in lignin degradation of OPFM bonds. The degraded lignin bonds and cellulose content in OPFM were proven by SEM, FTIR, and XRD.

Acknowledgment

This study was funded under the contract between the Directorate General of Higher Education, Research, and Technology Ministry of

Education, Culture, Research, and Technology, Indonesia, and Universitas Sriwijaya through the implementation of the state university operational assistance program for research in 2023 with contract no. 164/E5/PG.02.00.PL/2023.

REFERENCES

1. Baig, K.S., Wu, J., Turcotte, G., Doan, H.D. 2015. Novel ozonation technique to delignify wheat straw for biofuel production. Energy and Environment, 26(3), 303–318. https://doi.org/https://doi.org/10.1260/0958-305X.26.3.303
2. Baig, K.S. 2022. Kinetics of lignin removal from the lignocellulosic matrix after ozone transportation. Methane, 1(3), 177–188. https://doi.org/https://doi.org/10.3390/methane1030014
3. Barros, R. da R.O. de, Paredes, R. de S., Endo, T., Da Silva Bon, E.P., Lee, S.H. 2013. Association of wet disk milling and ozonolysis as pretreatment for enzymatic saccharification of sugarcane bagasse and straw. Bioresource Technology, 136, 288–294. https://doi.org/http://dx.doi.org/10.1016/j.biortech.2013.03.009
4. Bhattarai, S., Bottenus, D., Ivory, C.F., Haiming, A., Bule, M., Garcia-Perez, M., Chen, S. 2015. Bioresource technology simulation of the ozone pretreatment of wheat straw. Bioresource Technology, 196, 78–87. https://doi.org/10.1016/j.biortech.2015.07.022
5. Binder, A., Pelloni, L., Fiechter, A. 1980. Delignification of straw with ozone to enhance biodegradability. European Journal of Applied Microbiology and Biotechnology, 11(1), 1–5. https://doi.org/10.1007/BF00514070
6. Carolin C,F., Kamalesh, T., Kumar, P.S., Hemavathy, R.V., Rangasamy, G. 2023. A critical review on sustainable cellulose materials and its multifaceted applications. Industrial Crops and Products, 203, 1–19. https://doi.org/http://doi.org/10.1016/j.indcrop.2023.117221
7. Chieng, B.W., Lee, S.H., Ibrahim, N.A., Then, Y.Y., Loo, Y.Y. 2017. Isolation and characterization of cellulose nanocrystals from oil palm mesocarp fiber. Polymers, 9(8), 1–11. https://doi.org/https://doi.org/10.3390/polym9080355
8. Dwi Anggoro, D., Buchori, L., Kusuma Dewi, I., Prasetyaningrum, A. 2022. The effect of ozonation, ultrasonic, and hybrid ozonation-ultrasonic pretreatment methods on the delignification of oil palm mesocarp fibers. International Journal of Advanced Research, 10(12), 194–204. https://doi.org/https://doi.org/10.21474/ijar01/15827
9. Elanthikkal, S., Gopalakrishnapanicker, U., Varghese, S., Guthrie, J.T. 2010. Cellulose microfibres produced from banana plant wastes: Isolation and characterization. Carbohydrate Polymers, 80(3), 852–859. https://doi.org/10.1016/j.carbpol.2009.12.043
10. Fackler, K., Stevanic, J.S., Ters, T., Hinterstoisser, B., Schwanninger, M., Salmén, L. 2010. Localisation and characterisation of incipient brown-rot decay within spruce wood cell walls using FT-IR imaging microscopy. Enzyme and Microbial Technology, 47(6), 257–267. https://doi.org/10.1016/j.enzmictec.2010.07.009
11. Faix, O., Bremer, J., Schmidt, O., Tatjana, S.J. 1991. Monitoring of chemical changes in white-rot degraded beech wood by pyrolysis-gas chromatography and Fourier-transform infrared spectroscopy. Journal of Analytical and Applied Pyrolysis, 21, 147–162. https://doi.org/10.1016/0165-2370(91)80022-Z
12. García-Cubero, M.T., González-Benito, G., Indacoechea, I., Coca, M., Bolado, S. 2009. Effect of ozonolysis pretreatment on enzymatic digestibility of wheat and rye straw. Bioresource Technology, 100(4), 1608–1613. https://doi.org/10.1016/j.biortech.2008.09.012
13. García-cubero, M.T., Palacín, L.G., González-benito, G., Bolado, S., Lucas, S., Coca, M. 2012. An analysis of lignin removal in a fixed bed reactor by reaction of cereal straws with ozone. 107, 229–234. https://doi.org/10.1016/j.biortech.2011.12.010
14. Hermansyah, Cahyadi, H., Fatma, Miksusanti, Kasmiarti, G., Panagan, A.T. 2021. Delignification of lignocellulosic biomass sugarcane bagasse by using ozone as initial step to produce bioethanol. Polish Journal of Environmental Studies, 30(5), 4405–4411. https://doi.org/10.15244/pjoes/132263
15. Isroi, Ishola, M.M., Millati, R., Syamsiah, S., Cahyanto, M.N., Niklasson, C., Taherzadeh, M.J. 2012. Structural changes of oil palm empty fruit bunch (OPEFB) after fungal and phosphoric acid pretreatment. Molecules, 17(12), 14995–15012. https://doi.org/https://doi.org/10.3390/molecules171214995
16. Kamel, A., Al, H., Turcotte, G., Wu, J., Cheng, C. 2015. Ozone pretreatment of humid wheat straw for biofuel production. Energy Science & Engineering, 3(6), 541–548. https://doi.org/10.1002/ese3.93
17. Keris-Sen, U.D., Gurol, M.D. 2017. Using ozone for microalgal cell disruption to improve enzymatic saccharificatios of cellular carbohydrates. Biomass and Bioenergy, 105, 59–65. https://doi.org/10.1016/j.biombioe.2017.06.023
18. Lee, J.M., Jameel, H., Venditti, R.A. 2010. Effect of ozone and autohydrolysis pretreatments on enzymatic digestibility of coastal bermuda grass. BioResources, 5(2), 1084–1101. https://doi.org/10.15376/biores.5.2.1084-1101
19. Li, C., Wang, L., Chen, Z., Li, Y., Wang, R., Cai, G.,

Li, Y., Yu, Q., Lu, J. 2015. Ozonolysis pretreatment of maize stover: the interactive effect of sample particle size and moisture on ozonolysis process. Bioresource Technology. https://doi.org/10.1016/j.biortech.2015.01.042

20. Lim, M., Zulkifli, A.Z.S. 2018. Investigation of biomass surface modification using non-thermal plasma treatment. Plasma Science and Technology, 20(11), 115502. https://doi.org/10.1088/2058-6272/aac819
21. M'Arimi, M.M., Mecha, C.A., Kiprop, A.K., Ramkat, R. 2020. Recent trends in applications of advanced oxidation processes (AOPs) in bioenergy production: Review. Renewable and Sustainable Energy Reviews, 121, 1–18. https://doi.org/https://doi.org/10.1016/j.rser.2019.109669
22. Mardawati, E., Herliansah, H., Adillah, Q., Hanidah, I.I., Andoyo, R. 2018. Evaluation of ozonolysis pre-treatment for xylose production through enzymatic hydrolysis. AIP Conference Proceeding, 020080(September), https://doi.org/https://doi.org/10.1063/1.5055482
23. Neely, W.C. 1984. Factors affecting the pretreatment of biomass with gaseous ozone. Biotechnology and Bioengineering, 26(1), 59–65. https://doi.org/10.1002/bit.260260112
24. Pandey, K.K. 1999. A study of chemical structure of soft and hardwood and wood polymers by FTIR spectroscopy. Journal of Applied Polymer Science, 71(12), 1969–1975. https://doi.org/10.1002/(sici)1097-4628(19990321)71:12<1969::aid-app6>3.3.co;2-4
25. Schultz-Jensen, N., Leipold, F., Bindslev, H., Thomsen, A.B. 2011. Plasma-assisted pretreatment of wheat straw. Applied Biochemistry and Biotechnology, 163(4), 558–572. https://doi.org/10.1007/s12010-010-9062-5
26. Schwanninger, M., Rodrigues, J.C., Pereira, H., Hinterstoisser, B. 2004. Effects of short-time vibratory ball milling on the shape of FT-IR spectra of wood and cellulose. Vibrational Spectroscopy, 36(1), 23–40. https://doi.org/10.1016/j.vibspec.2004.02.003
27. Sharma, S. das, Pugsley, T.S. 2007. Effect of particle size distribution on the performance of a catalytic fluidized bed reactor. 12th International Conference on Fluidization, 655–662.
28. Shi, F., Xiang, H., Li, Y. 2015. Combined pretreatment using ozonolysis and ball milling to improve enzymatic saccharification of corn straw. Bioresource Technology, 179, 444–451. https://doi.org/http://dx.doi.org/10.1016/j.biortech.2014.12.063
29. Shrestha, R., Joshi, U.M., Subedi, D.P. 2015. Experimental study of ozone generation by atmospheric pressure dielectric barrier discharge. International Journal of Research and Review, 8(4), 24–29.
30. Simão, J.A., Marconcini, J.M., Capparelli Mattoso, L.H., Sanadi, A.R. 2019. Effect of SEBS-MA and MAPP as coupling agent on the thermal and mechanical properties in highly filled composites of oil palm Fiber/PP. Composite Interfaces, 26(8), 699–709. https://doi.org/10.1080/09276440.2018.1530916
31. Sreekala, M.S., Kumaran, M.G., Thomas, S. 1997. Oil palm fibers: morphology, chemical composition, surface modification, and mechanical properties. Journal of Applied Polymer Science, 66(5), 821–835. https://doi.org/10.1002/(sici)1097-4628(19971031)66:5<821::aid-app2>3.0.co;2-x
32. Suhada, N., Rasid, A., Shamjuddin, A., Aishah, N., Amin, S. 2021. Chemical and structural changes of ozonated empty fruit bunch (EFB) in a ribbon-mixer reactor. 16(2), 383–395. https://doi.org/10.9767/bcrec.16.2.10506.383-395
33. Sulfahri, Mushlihah, S., Langford, A., Tassakka, A.C.M.A.R. 2020. Ozonolysis as an effective pretreatment strategy for bioethanol production from marine algae. Bioenergy Research, 13(4), 1269–1279. https://doi.org/10.1007/s12155-020-10131-w
34. Travaini, R., Marangon-Jardim, C., Colodette, J.L., Morales-Otero, M., Bolado-Rodríguez, S. 2015. Ozonolysis. In pretreatment of biomass: Processes and technologies, 105–135. Elsevier B.V. https://doi.org/10.1016/B978-0-12-800080-9.00007-4
35. Travaini, Rodolfo, Barrado, E., Bolado-Rodríguez, S. 2016. Effect of Ozonolysis pretreatment parameters on the sugar release, ozone consumption and ethanol production from sugarcane bagasse. Bioresource Technology, 214, 150–158. https://doi.org/10.1016/j.biortech.2016.04.102
36. Travaini, Rodolfo, Otero, M.D.M., Coca, M., Da-Silva, R., Bolado, S. 2013. Sugarcane bagasse ozonolysis pretreatment: Effect on enzymatic digestibility and inhibitory compound formation. Bioresource Technology, 133, 332–339. https://doi.org/10.1016/j.biortech.2013.01.133
37. United State Department of Agriculture. 2023. Indonesia Palm Oil: Historical Revisions Using Satelite-Derived Methodology. In COmmodity Intelligence Report. https://ipad.fas.usda.gov/highlights/2012/08/Mexico_corn/
38. Valdés, H., Sánchez-Polo, M., Rivera-Utrilla, J., Zaror, C.A. 2002. Effect of ozone treatment on surface properties of activated carbon. Langmuir, 18(6), 2111–2116. https://doi.org/https://doi.org/10.1021/la010920a
39. Vanderfleet, O.M., Cranston, E.D. 2021. Production routes to tailor the performance of cellulose nanocrystals. Nature Reviews Materials, 6(2), 124–144. https://doi.org/10.1038/s41578-020-00239-y
40. Vitasari, D. 2008. The Effect of Ozone Concentration on the Bleached Pulp Properties. Seminar Nasional Teknoin 2008 Bidang Teknik Kimia Dan Tekstil, 17–21.
41. Wan Omar, W.N.N., Amin, N.A.S. 2016. Multi response optimization of oil palm frond pretreatment

by ozonolysis. Industrial Crops & Products, 85, 389–402. https://doi.org/10.1016/j.indcrop.2016.01.027

42. Wan Omar, W.N.N., Saidina Amin, N.A. 2021. Fractionation of oil palm fronds (OPF) by ozonolysis for enhanced sugar production. Chemical Engineering Transactions, 83, 409–414. https://doi.org/10.3303/CET2183069
43. Wan, X., Ping, Y., Li, J. 2021. Effect of ozone treatment on the properties of oil palm empty fruit bunch sulfonated chemi-mechanical pulp. Forests, 12(8), 1–12. https://doi.org/http://doi.org/10.3390/f12081085
44. Yasim-Anuar, T.A.T., Ariffin, H., Norrrahim, M.N.F., Hassan, M.A. 2017. Factors affecting spinnability of oil palm mesocarp fiber cellulose solution for the production of microfiber. BioResources, 12(1), 715–734. https://doi.org/10.15376/biores.12.1.715-734
45. Yulianto, E., Restiwijaya, M., Sasmita, E., Arianto, F., Kinandana, A.W., Nur, M. 2019. Power analysis of ozone generator for high capacity production. Journal of Physics: Conference Series, 1170(1). https://doi.org/https://doi.org/10.1088/1742-6596/1170/1/012013